Chapter 7
Powder-Mixed Microelectric Discharge Machining

Basil Kuriachen

Abstract Microelectric discharge machining (µEDM) is introduced to the manufacturing industry to produce microfeatures and microholes on difficult to machining materials such as titanium- and nickel-based alloys and other heat-resistant electrically conductive metals and alloys. Even though µEDM can be used to machine any electrically conductive materials, there are many problems to be addressed in order to make it as an accurate and reliable process. Some of the problems associated are low material removal rate, tool wear rate, high surface roughness, and poor dimensional accuracy. This chapter presents powder-mixed microelectric discharge machining as one of the viable alternatives to overcome some of the inherent difficulties associated with microelectric discharge machining process. Suspension of electrically conductive and semiconductive powders in the dielectric can strongly influence the process in a desirable manner. Moreover, the added powder particle gets re-solidified along with the tool material on the machined surface and opens a new possibility to modify the machined surface by selecting the appropriate alloying elements in the required proposition. This approach needs to be thoroughly addressed to explore as 'µEDM alloying'.

Keywords Powder-mixed µEDM · µEDM alloying · Material removal rate
Surface modification · Surface roughness · Inter-electrode gap · Tool wear rate

7.1 Introduction

In the last few decades, materials with unique mechanical and metallurgical properties like titanium, nickel, cobalt, and other heat-resistant superalloys as well as MMCs were developed to meet the extreme applications in aerospace and various other industries. In addition, miniaturization is no more a fashion; rather, it is the

B. Kuriachen (✉)
Mechanical Engineering Department, National Institute of Technology Mizoram, Aizawl 796012, Mizoram, India
e-mail: basilkuriachen@gmail.com

need of the hour due to less material and space requirements. Micromachining is a value-adding element for many capacities where size reduction harvests economic and technical aids. In order to keep alongside with sophisticated microparts design on difficult to machine materials, microelectric discharge machining (μEDM) is proved to be an effective and viable alternative to produce complex three-dimensional components. However, the performance of μEDM in terms of machining speed, MRR, and surface finish needs to be improved to meet the productivity challenges. Therefore, researchers have suggested that suspension of micro-/nanoparticles in the dielectric medium during microelectric discharge machining has several advantageous in improving the process capabilities and to produce sound machined surface. This chapter presents the working principle, mechanism of material removal, important electrical and non-electrical parameters, effect of powder on various machining responses as well as on machined surfaces.

7.2 Working Principle

The material removal mechanism of electric discharge machining (EDM) and μEDM is similar except in the discharge energy and the size of the features produced. Generally, EDM machining of microfeatures of size in the range of 1–1000 μm and discharge energy less than 1000 μJ is considered as microelectric discharge machining (μEDM). The basic scheme of microelectric discharge machining can be illustrated as shown in Fig. 7.1. The electrodes are connected to a suitable DC electric power and separated by an inter-electrode gap (IEG) based on servo voltage and maintained throughout the machining. The workpiece and the tool are either submerged in dielectric or a forced circulation of dielectric using an external pumping mechanism is used. Generally, deionized water, kerosene, or paraffin oils are used as the dielectric fluid. The continuous circulation of dielectric helps to improve the flushing efficiency of the dielectric fluid. Hence, it is preferred. Once, a suitable electric supply is established, the dielectric breakdown takes place and sparks are generated.

Fig. 7.1 Basic scheme of electric discharge machining
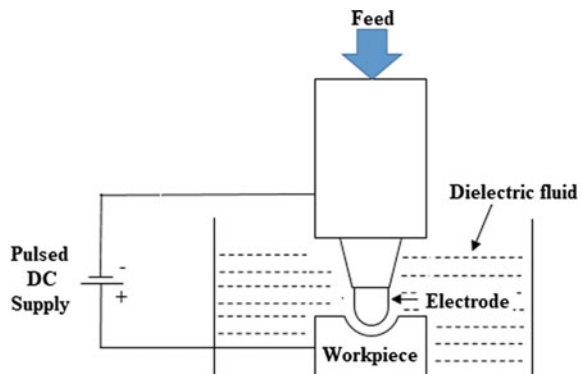
The heat energy produced as a result of electric sparks liquefy and evaporate a minor percentage of electrodes (both tool and workpiece). Hence, the working principle of μEDM/EDM can be named as localized melting and vaporization.

Explanation of a typical microelectric spark is a difficult task as it exists only for fraction of micro- or nanoseconds as well as size reduction. Moreover, application of hydrodynamics, thermodynamics, and other several theories of science and engineering made the process become more versatile. Hence, it is not an easy task to enlighten the mechanism of electric spark in μEDM. Many theories have been proposed by researchers and available in the literature and divided into electrothermal and electromechanical models. In the first theory, the removal of material takes place due to the localized melting and vaporization as results of heat transfer from the superheated plasma channel established between the tool and workpiece, whereas, in the second model, it is considered yielding as the main mechanism of erosion. It is explained that the workpiece is subjected to an electrostatic force which instigates stress, and localized area higher than the yield strength is dislodged. From the two theories, electrothermal theory is broadly accepted due to the fact that it can explain many of the practical phenomena associated with the EDM/μEDM/PMμEDM material removal. Hence, electrothermal theory for material removal is explained in detail. In a typical EDM spark as shown in Fig. 7.2, electrons are ejected from the cathode and gain momentum towards anode under the influence of electric potential. These electrons get bombarded with dielectric molecules, neutral atoms and split the molecules into positively charged ions and negatively charged electrons; thereby, an avalanche of electrons and ions is formed. All the electrons formed in the inter-electrode gap (IEG) get accelerated towards the anode (workpiece), and ions get accelerated to the cathode (tool electrode); thereby, a plasma channel is established between the tool and workpiece. This results in the breakdown of IEG. As a result of the high temperature and pressure developed on the plasma channel, gas bubbles are produced. The pressure within these bubbles is reported as 6–14 bar. It accelerates the superheating. The difference in pressure inside and outside of the bubbles results in cavitation during the breakdown, and molten metal gets expelled. Also, the dielectric surges back into the plasma. Sudden elimination of the plasma and some molten metal remain as re-solidified layer on the workpiece.

The application of powder particle into the dielectric medium is one of the developments to improve the processes capabilities of μEDM. Even though the working principle is similar to μEDM, it has a different mechanism of sparking phenomena. Once the powder particle mixed with the dielectric, the IEG pollution with powder particle in the dielectric takes place. The conductive or semiconductive particle in IEG gets energized during the application of electric potential as shown in Fig. 7.3. It acts as a conductive column between the tool and electrode and workpiece. This improves the dielectric strength of the dielectric fluid. This formation of conductive column of powder promotes the discharge of capacitor before attaining the full charge and the required voltage. This enhances the early discharge and reduces the discharge energy per sparks. Moreover, the energy gets distributed among the workpiece, tool, and dielectric more effectively, thereby produces small diameter crater with more consistency throughout the machined surface. This is not only improving the flushing
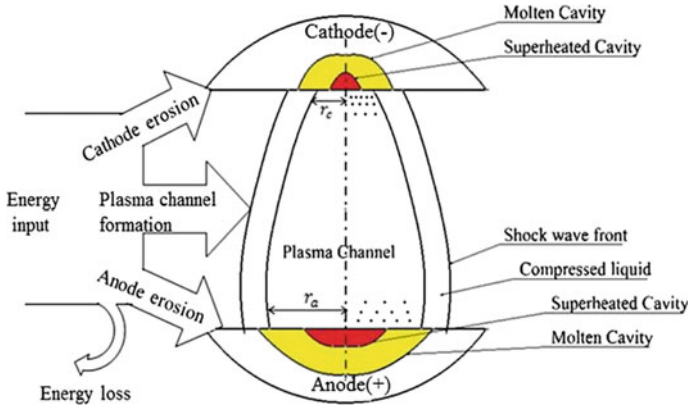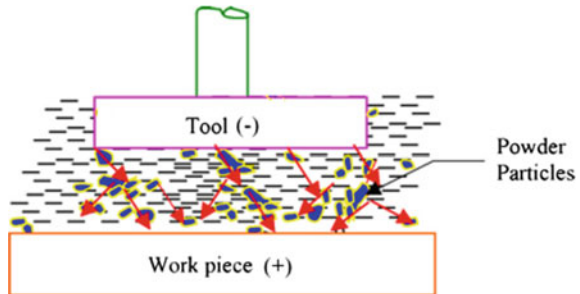
Fig. 7.2 Schematic diagram of EDM spark

Fig. 7.3 Principle of PMμEDM [1]

efficiency but also surface finish [1–4]. In addition, the micro-/nanopowder particles in the IEG also get melted along with the tool and workpiece as well as get solidify on the machined surface along with the electrode material. The melting and re-solidification also depend on the discharge energy which mainly depends on the pulse generation used in the circuit.

7.3　Pulse Generator

RC circuit as shown in Fig. 7.4 was used in EDM equipment in the early stages of its invention. This was replaced by power transistors as shown in Fig. 7.5 which is generally used in conventional EDM machines due to its capabilities to generate high pulse duration [5]. Even though RC pulse generators are used in μEDM due to the possibilities to obtain significantly short pulse duration with consistent discharge energies [5], Jahan et al. [6] have studied and compared the effects of relaxation-type and transistor-type pulse generators in micro-ED machining of tungsten carbide and concluded that relaxation type is more suitable for micromachining applications
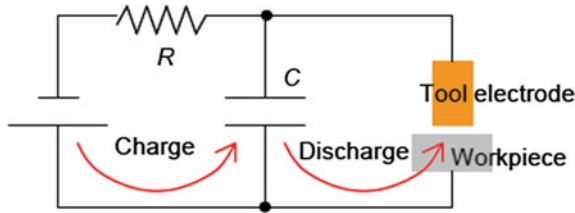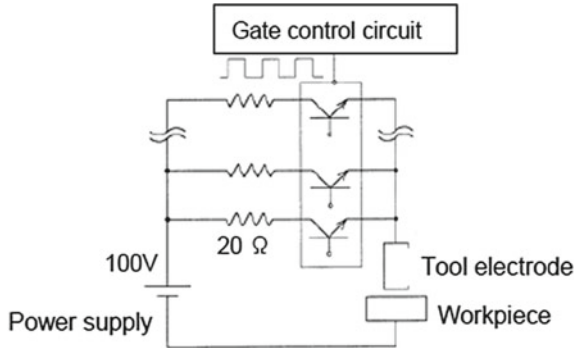
Fig. 7.4 Relaxation-type pulse generator [5]

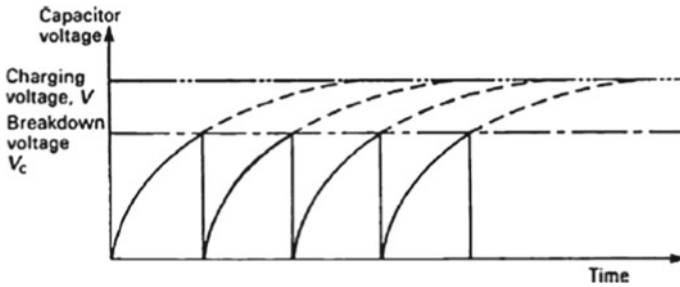
Fig. 7.5 Transistor-type pulse generator [5]

Fig. 7.6 Variation of capacitor voltage with time in *RC* circuit [7]

because of its capability to reduce the pulse energy per sparks. In *RC* type at low resistance, a primary release of energy will follow, but if it is large, the capacitor will accomplish an upper charge before the discharge occurs [7]. Figure 7.6 shows the variation of instantaneous voltage in the inter-electrode gap with time in *RC* circuit. As observed from Fig. 7.4, the capacitor gets charged from the DC source (*V*) through the resistance (*R*). The instantaneous voltage across the IEG follows the relation

$$V_i = V\left(1 - e^{-\frac{t}{RC}}\right) \tag{7.1}$$

where 't' is the time at the instant 'V' is applied. R and C are the resistance and capacitance value of the discharge circuit. As shown in Fig. 7.6, the 'V_i' tries to approaches to 'V' if allowed. However, the inter-electrode gap (through servo control mechanism), tool electrode, and dielectric medium, etc., are adjusted in such a way to discharge the capacitor, while the 'V_i' reaches the discharge voltage 'V_c' At this instance, the complete discharge of the capacitor takes place and the energy released into the inter-electrode gap which is equal to

$$E_d = \frac{1}{2}CV_d^2 \tag{7.2}$$

The major portion of the machining time is used to charge the capacitor after each discharge, whereas the discharge time 't_d' is approximately (10%) of the charging time 't_c'. Hence, the heat flux incident on the surface of the workpiece can be calculated as follows

$$Q_i = \frac{E_d}{t_d} \tag{7.3}$$

where t_d is the discharge time in which the actual spark takes place. The total discharged heat is scattered between the workpiece, tool, and dielectric. Majority of the heat energy is carried away by the dielectric fluid. Hence, only a small portion of heat is available on the workpiece for the removal of material. This is represented by 'η'. Therefore, the available heat flux for removal of material can be calculated as follows

$$Q_a = \eta Q \tag{7.4}$$

where Q_a is the heat flux incident on the anode. The heat flux density can be calculated as

$$q = \frac{Q_a}{\pi r_s^2} \tag{7.5}$$

where r_s is the spark radius. The heat flux distribution for the removal of material from μEDM can be written by adopting Gaussian distribution of heat flux as follows

$$q_r = 3.157 q e^{-3\left(\frac{r}{r_s}\right)^2} \tag{7.6}$$

The influence of suspended particle in the dielectric can be incorporated in Eq. 7.6 by introducing a new parameter 'K_n'.

$$q_r = K_n 3.157 \frac{\eta Q}{\pi r_s^2} e^{-3\left(\frac{r}{r_s}\right)^2} \tag{7.7}$$

where 'K_n' depends on the size, type, and % of particles in the dielectric. For graphite powder of 30 μm average diameter, frequency constant 'K_n' is considered as 2.4. Moreover, the electric discharge mechanism in powder-mixed μEDM depends on various process parameters, and it can be broadly classified into electrical and non-electrical parameters.

7.4 PMμEDM Process Parameters

The independent variables of PMμEDM can be classified into two, i.e. electrical and non-electrical parameters as depicted in Fig. 7.7.

7.4.1 Electrical Parameters

Important variables under this category are voltage, capacitance, current, pulse off time, pulse on time, polarity, and pulse waveform. Discharge voltage is depended on spark gap and breakdown strength of the working fluid. The open gap voltage increases until the discharge (ionization path between electrodes) occurs through the dielectric. Once the current starts to flow through the inter-electrode gap (discharge starts), voltage drops and stabilizes at the working gap. This voltage regulates the IEG between the leading edges of the electrode and workpiece. Therefore, an upper voltage setting increases the inter-electrode gap, which in turn progresses the flushing settings as well as supports to become stable the machining [8, 9]. Increase in open-circuit voltage increases the MRR, electrode wear ratio (RWR) and SR due to the increase in electric field strength. Jahan et al. [10] have been experimentally
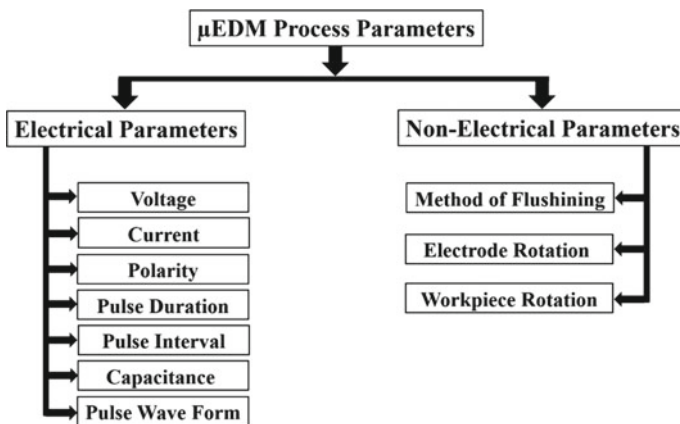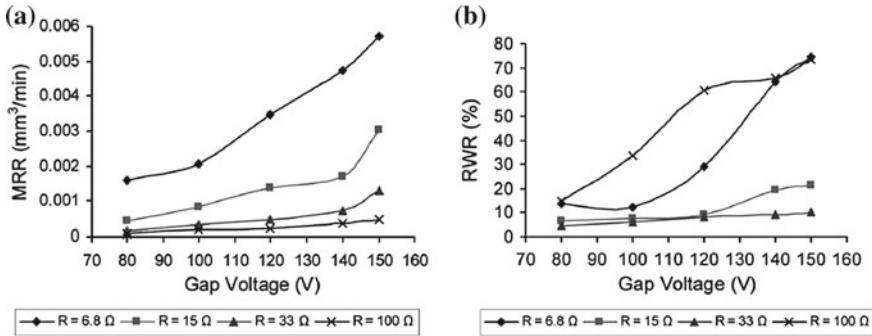

Fig. 7.7 μEDM parameters

Fig. 7.8 Variation of **a** MRR, **b** RWR with respect to voltage [11]
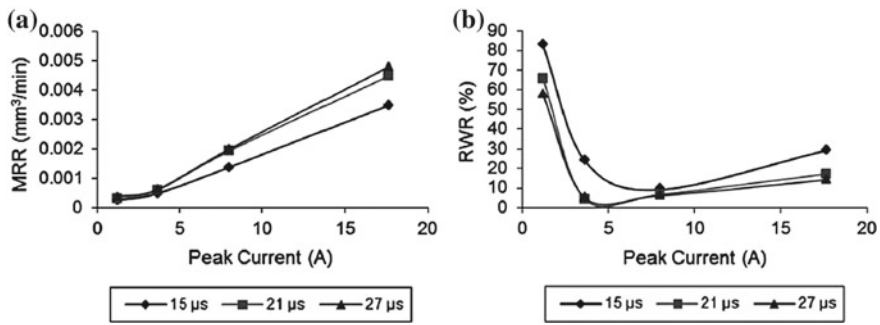

Fig. 7.9 Variation of current on **a** material removal rate, **b** RWR during µEDM of tungsten carbide [11]

investigated the influence of gap voltage during the micro-ED drilling of cemented carbides using tungsten electrodes, and effect of voltage on EWR and MRR at various resistance is shown in Fig. 7.8.

Another significant electrical parameter is current in microelectrical discharge machining. It is the quantity of current used during machining and measured in amperage. For each pulse, it surges until it reaches the required level, which is expressed as the peak current. The all-out amount of the current is decided by the surface area of the cut. During roughing operation, upper value of current is used which gives better MRR. The setting of peak current in EDM is important because the machined cavity is exact replica of the tool. Graphite and other improved tool materials can work on higher peak current without much damage [12]. The variation of material removal rate and RWR is depicted in Fig. 7.9.

Pulse duration is also known as pulse on time. It is the time in which the energy is applied and measured in microseconds. The duration of the pulse and the frequency of pulse are important as the actual work is done during the pulse on time. With longer pulse, the energy applied is high; the amount of material gets melted also will be increased. The size of the crater formed is broader and deeper in the short pulse
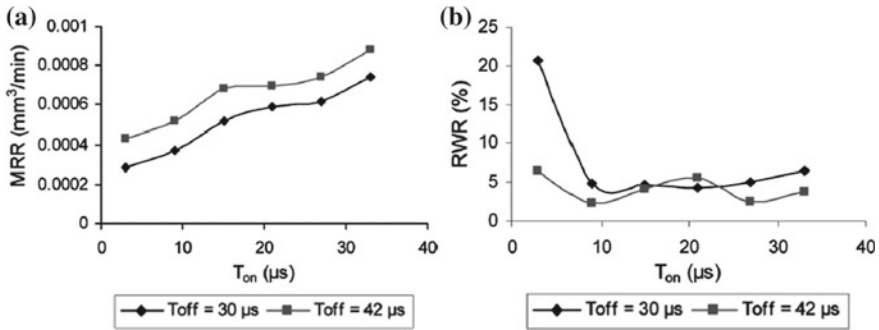
Fig. 7.10 Variation of **a** material removal rate, **b** RWR of tungsten carbide with respect to discharge time [11]

on time. This in turn increases the surface roughness, and prolonged sparking time allows more energy to absorb into the electrodes, thereby results in increased recast and HAZ zone [7, 10]. Figure 7.10 illustrates the variation of sparking time with respect to MRR and RWR.

In *RC* circuit, the pulse energy is mainly depending on the discharge voltage and capacitance. The maximum energy per pulse is obtained by Eq. 7.2. The effect of voltage is discussed in the previous sections. In *RC* circuit, the capacitance decides the pulse on time and its frequency of discharging [6]. Jahan et al. [6] investigated the effect of capacitance on the performance of μEDM and found that with an increase in capacitance, the MRR increased due to the increase in the discharge energy. As the capacitance increase, the discharge current also increases which results in deep crater.

Polarity of the workpiece can be fixed as either positive or negative. The plasma channel created between the workpiece and electrode is composed of both electrons and ions. The momentum of electrons is higher than ions due to light in weight compared to ions. The electrons possess quicker action in the plasma channel and convert the kinetic energy on the anode, and maximum material removal took place, whereas ions move relatively slower than electrons and converts less energy in the cathode; thereby, less material removal takes place in cathode. However, while running longer discharges, the early electron process predominance charges to positron process, resulting in cathode wear. So, polarity of the electrodes is generally determined by experiments and is a matter of tool material, work material, current density, and pulse length combinations [7]. The wrong selection of polarity can have significant implications on speed, wear, and stability of machining [13, 14]. Some of the general polarity guide lines are listed in Table 7.1. Due to the faster-accelerating electron in the plasma channel, the material removal volume in single discharge is higher at the anode compared to the volume at the cathode. This effect is known as polarity effect [14]. Figure 7.11 shows the comparison of electrode wear in boron-doped CVD-diamond (B-CVD) as electrode at positive and negative polarity. B-CVD

Table 7.1 General polarity guidelines [13]

Tool	Workpiece	Remarks
Graphite (+)	Steel (−)	General purpose
Graphite (−)	Steel (+)	High speed and 20% wear
Graphite (−)	Copper (+)	General purpose
Copper tungsten (+)	Steel (−)	General purpose
Copper tungsten (+)	Carbide (−)	General purpose

leads to fifty times higher wear with positive polarity than with negative polarity. The machining time also increased simultaneously by more than 200%.

Pulse interval is also known as the pulse off time. It is the time, in which the machining (or sparks) does not occur. It affects the machining speed, stability, and the machined surface. The melted workpiece (debris) during the pulse on time is ejected and flushed away with the dielectric fluid during pulse off time. The machining operation is faster at shorter interval as shown in Fig. 7.12. But, if the off time is too short, the debris will not have flushed away effectively and increase the chance to occur secondary sparking as well as prolonged machining time and reduce the material removal rate.

The pulse waveform is generally rectangular; however, pulse with various other forms is also used for electric discharges. Generators with trapezoidal pulses can reduce the comparative wear of cathode (generally tool) to small values. The actual profile of a single EDM pulse is as shown in Fig. 7.13.

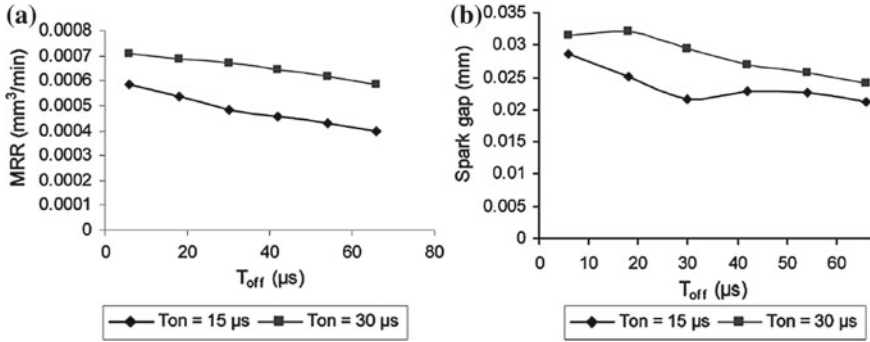**Fig. 7.11** Comparison of tool polarity and electrode relative wear [14]
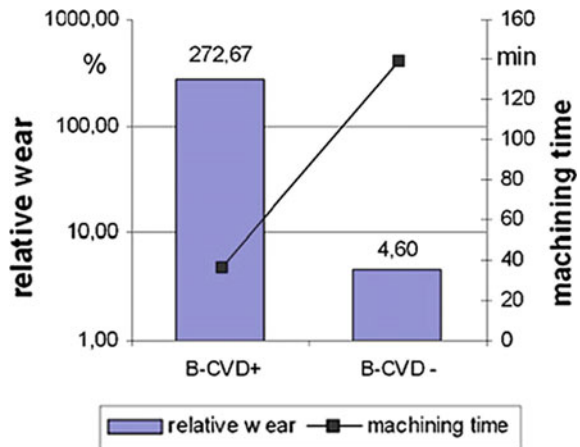
Fig. 7.12 Variation of pulse on and off time on **a** MRR, **b** spark gap during micro-EDM of WC-Co [11]
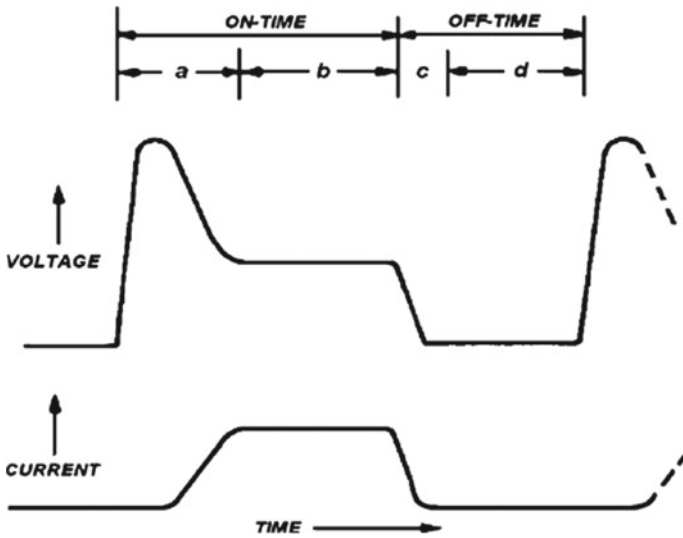

Fig. 7.13 Actual pulse of a single EDM pulse [15]

7.4.2 Non-electrical Parameters

Non-electrical parameters have also significant effect on machining and optimizing performance measures like electrical parameters. The main non-electrical parameters include flushing and electrode rotation along with powder concentration.

Dielectric flushing is important in electrical discharge machining. The dielectric fluid should have the basic characteristics such as high dielectric strength and swift recapture after breakdown and flushing capability. MRR, TWR, and recast layer are exaggerated by the dielectric fluid and technique used for flushing [7, 16]. The flushing flow rate plays important role in crack density in the machined surface

which can be minimized by optimum flushing rate [16]. Kerosene, deionized water, and hydrocarbon oils are used as dielectric fluid. Among them, hydrocarbon oils and kerosene decompose during machining and deposit carbon on the machined surface. Deionized water is used where the carbon-free surfaces need to be produced.

Electrode rotation helps to generate favourable centrifugal forces in the fluid and flush away the debris from the inter-electrode gap effectively. Electrode rotation causes two things on the dielectric fluid. Firstly, it creates a centrifugal force on the dielectric fluid and pulls out the unwanted materials. Secondly, it creates some turbulence in the fluid which allows the fresh fluid to enter in the gap and wash away the particles [17]. Hence, improvements in the machining responses have been reported due to effective flushing and electrode rotation [10].

7.5 Effect of Powder on IEG

The suspension of powder in the dielectric fluid enlarges the inter-electrode gap. As discussed earlier, the inter-electrode gap is influenced by voltage, flushing methods, dielectric, etc. The studies showed that increase in the powder concentration increases the inter-electrode gap [18]. Figure 7.14 shows the enlargement of hole diameter against the increase in the powder concentration in the dielectric fluid as well as comparison of dielectric fluid mixed with dielectric fluid mixed with silicon, aluminium, and pure dielectric fluid. As evident from Fig. 7.15, the increase in the powder concentration increases the additional gap pollution which leads to the high probability to occur the primary discharge between the tool and powder particles instead of tool and workpiece. This is due to the fact that the conductive or semi-conductive powder particles get energized and reduce the effective discharge gap (distance between the tool and powder particles), thereby reduces the breakdown voltage under the influence of electric field in the IEG. Hence, the early discharge of capacitance (before full charging) takes place, and secondary sparks may exist between the powder particles and workpiece; thereby, the inter-electrode gap gets increases compared to pure dielectric. The magnitude of increase in IEG depends on the variation of material and electrical properties of the powder particles suspended in the dielectric. In case of pure dielectric fluid, there is no additional gap pollution (other than with debris) between the tool and workpiece and the discharge takes place between the tool and workpiece. Hence, the inter-electrode gap is comparatively larger in PMμEDM compared to μEDM.

7.6 Effect of Powder on MRR

The variation of machining responses is widely depending on the type and material properties of the powder particles. Kuriachen and Mathew [1] have conducted a study on the effect of powder (SiC) suspension in the dielectric on material removal rate
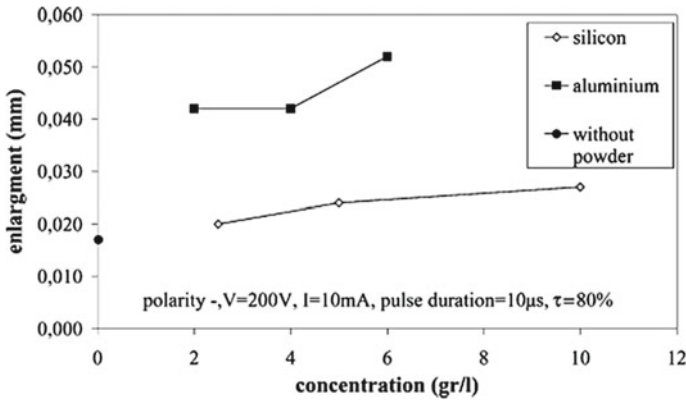
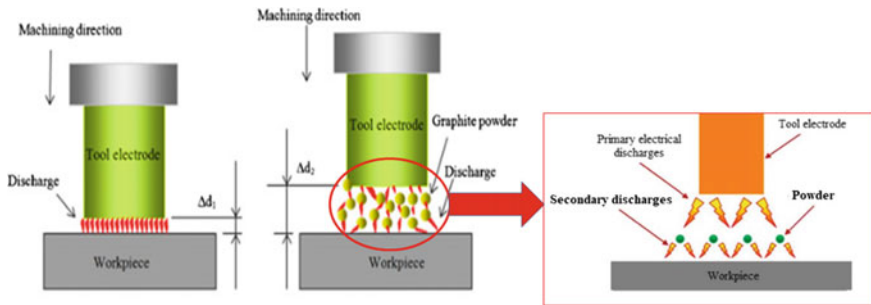**Fig. 7.14** Variation of IEG with powder concentration during PMμEDM [18]

Fig. 7.15 Comparison of sparking phenomena in μEDM and PMμEDM [19, 20]

(MRR). From the results reported, the material removal rate found to increase when the semiconductive particle concentration (SiC) varied from 5 to 25 g/L. However, the variation with respect to capacitance and voltage showed a different trend. Initially, i.e. variation of 5–15 g/L of powder concentration increased MRR; thereafter, it found to be decreasing. This is due to the fact that increase in powder concentration increases the IEG pollution with SiC which improves the bridging of the discharge gap between the electrodes. Due to this bridging effect, the insulating strength of the dielectric decreases. Hence, the chance of easy short circuit takes place. It results in early explosion of discharges [9]. Hence, early discharge of the partially charged capacitor takes place; i.e. the capacitor may not get charged fully. It results in the reduction of discharge energy release into the IEG. Therefore, the amount of material removed also reduces proportionally. Secondly, once the short circuit happens, the tool moves backward and searches for new optimum gap to start with new sparks. This results in the increase in machining time to complete the required machining cavity. This in turn reduces the MRR.

On the contrary, Prihandana et al. [21] reported that suspension of micro-MoS_2 powder in the dielectric increases the material removal rate as shown in Fig. 7.16.
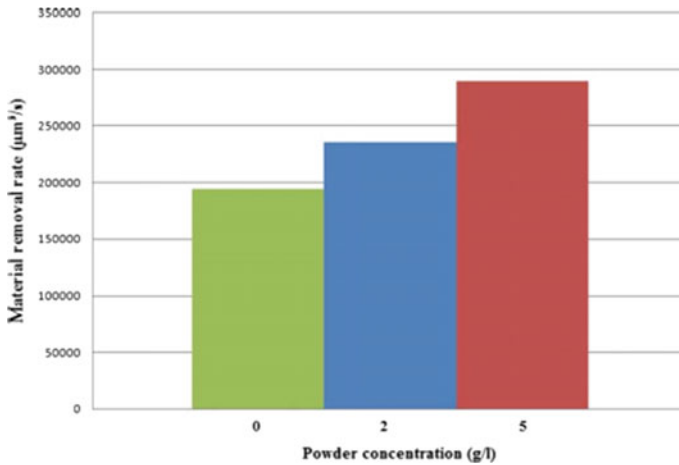
Fig. 7.16 Variation of MRR with respect to powder concentration [21]

It can be clearly understood that high concentration of powder (5%-micro-MoS$_2$) particles increases the material removal rate compared to 2 and 0% powder in the dielectric. It is due to the semiconductor property of the powder particles; thereby, the dielectric strength of the fluid is reduced and increased the inter-electrode gap. The increase in IEG along with high powder concentration in IEG reduces the adhesion of the particles to the tool and workpiece, thereby reduces the chances of bridging of IEG. This results in the reduction of short circuiting and reduces the machining time and increases the MRR [21, 22]. Therefore, it can be concluded that the effect of powder on the MRR not only depends on the powder concentration in the dielectric but also depends on the type, material, and electric properties of the tool.

7.7   Effect of Powder on Tool Wear Rate

Effect of powder concentration in dielectric on the tool wear shown that increase in powder concentration increases the tool wear. Due to the presence of less powder particle in the IEG at low level of powder concentration (5 g/L), the proportion of energy available at the cathode for removal is less in contrast to anode. Therefore, small amount of material gets removed at low level of powder concentration. At higher level of powder concentration (25 g/L), the existence of redundant amount of powder leads to unstable electric discharge [10]. At the interaction of voltage and powder concentration at higher levels, the maximum amount of material found to be removed from the tool electrode [1, 23].

7.8   Effect of Powder on Machining Time

As discussed in the Sect. 7.6, the pure dielectric fluid with relatively low flow rate in the narrow IEG increases the chances of adhesion of debris in the IEG whereby the bridging and short-circuiting take place. Once short circuiting is detected by the servo control mechanism, the tool retracts in the reverse direction and searches for a new optimum IEG as depicted in Fig. 7.17. This results in increased machining time and reduces machining efficiency. Studies reported by Prihandana et al. [19] with the suspension of graphite particles in the dielectric as shown in Fig. 7.18, with increase in powder concentration (graphite) 0–10%, the machining time reduced by 14–20 times faster. This is interpreted as the 10 g/l of graphite powder in the dielectric effectively bridge the IEG thereby frequency of quality discharge increases thus the machining time [19].
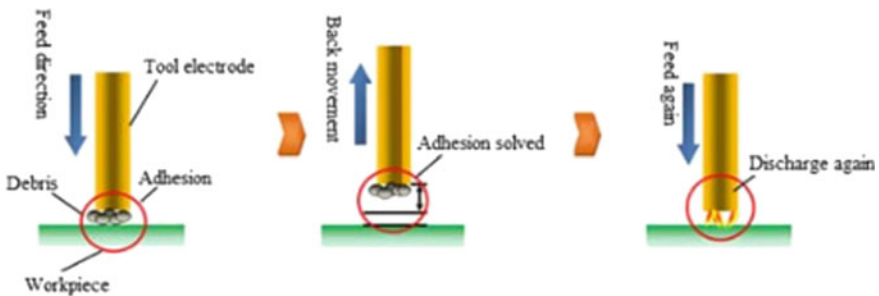

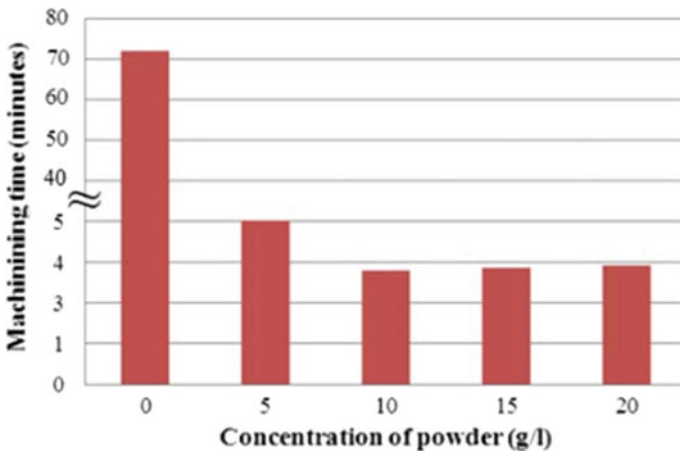**Fig. 7.17**   Effect of adhesion on machining stability [19]

Fig. 7.18   Variation of machining time with respect to graphite powder concentration [19]

7.9 Effect of Powder on Surface Roughness

Unlike material removal rate, the increase in powder concentration in the dielectric reduces the surface roughness and improves the surface finish as shown in Fig. 7.19. Beyond the scope of the type and material properties of powders, all the conductive or semiconductive powder in dielectric decreases the surface roughness and improves the surface finish. Researcher's explained this trend is due to the fact that increase in powder concentration increases the number of powder particles in the IEG. These particles get energized as discussed earlier and produce the spark between the tool and
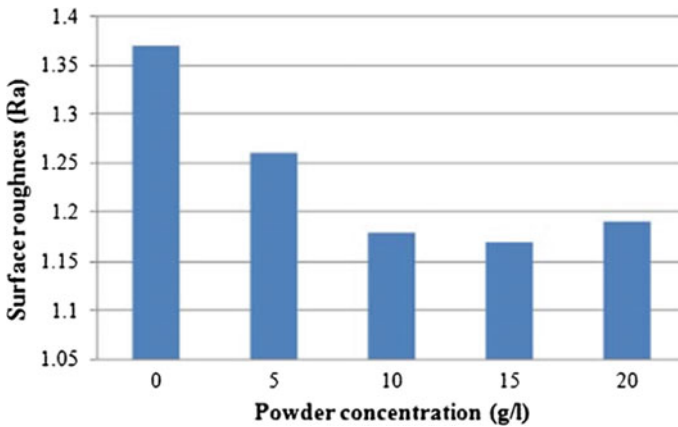

Fig. 7.19 Variation of surface roughness with powder concentration [19]
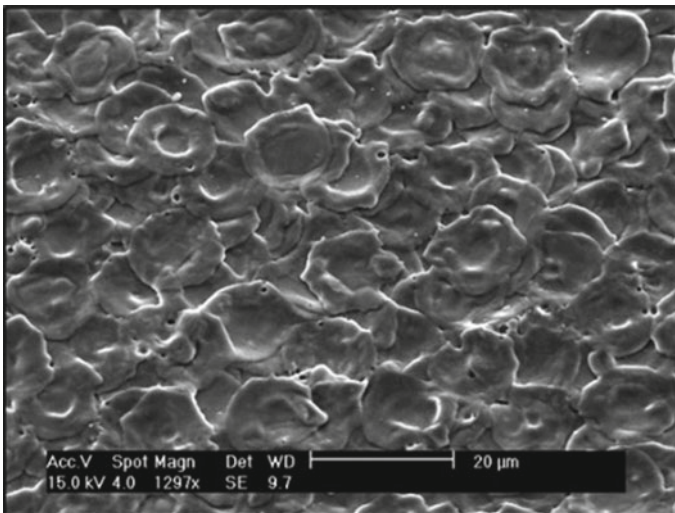

Fig. 7.20 SEM image of the graphite PMμED machined surface [19]

powder particle as well as with the powder and workpiece (secondary sparks). This reduces the intensity of sparks, thereby produces low intensive and more uniform craters on the machined surface instead of high intensive shallow craters for the same discharge energy as shown in Fig. 7.20. This phenomenon results in the reduction of R_a and R_{max} (surface roughness) of the produced surface.

7.10 Effect of Powder on Machined Surface

Researchers have established and proved that some of the melted material get re-solidify on the machined surface due to the cooling effect of dielectric fluid. This is more relevant in the case of powder PMμEDM due to the enhancement of the thermal conductivity of the fluid. Kuriachen [23] have investigated the possibility
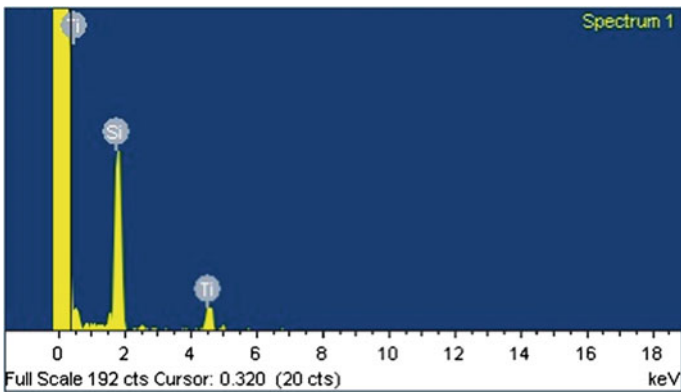
(a) EDS composition analysis of μPAMEDM processed Ti-6Al-4V surface
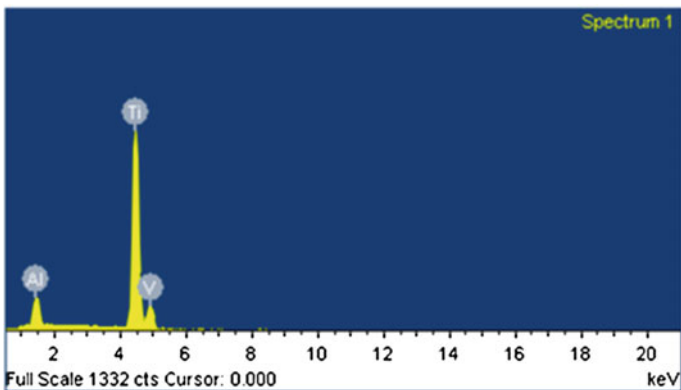
(b) EDS composition analysis of unprocessed Ti-6Al-4V surface

Fig. 7.21 EDS composition analysis [1]

Fig. 7.22 SEM images of the microslot at a capacitance of 0.1 µF, voltage of 115 V, and powder concentration of 15 g/L [1]
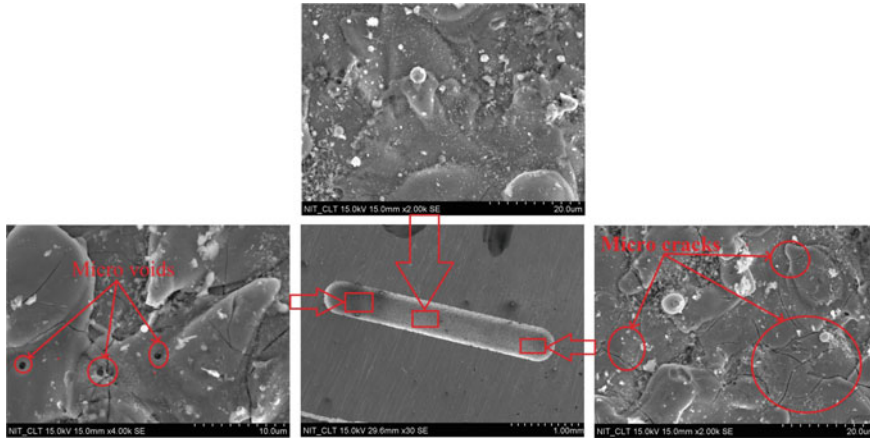
of developing microelectric discharge alloying by suspending SiC powder in the dielectric. Analysis of the machined surface (Fig. 7.22) of titanium alloy confirms the existence of a thin re-solidified layer. It was also found that microcracks, small pits, residues of recast, etc., are identified towards the end of the microchannel machined. However, only a few microcracks are observed at the centre of the channel. This is reported as the fact that tool remains more time towards the ends of the microchannel. Hence, more thermal residual stress is experienced. Further analysis through EDX revealed (Fig. 7.21) that silicon material gets migrated on to the machined surface, whereas it was not present on the unprocessed surface. In addition to silicon, the residuals of the tool material are also detected on the machined surface. Hence, the material from tool and dielectric is present in the plasma, and a small portion gets solidify on the machined surface. Moreover, the surface properties also get altered due to the frequent heating and cooling cycles. The microhardness of the machined surface gets increased. It was reported that 100% improvement in the micro hardness of the powder EDMed surface [24].

Prihandana et al. [21] studied the effect of MoS_2 micropowder in the dielectric along with ultrasonic vibration on the mechanical surface. The comparison of pure dielectric mixed with micro-MoS_2 particle revealed that a significant difference in quality of the surface is produced. The machined surface with pure dielectric shown a significant deposition of carbon particles at the centre of the blind microhole produced as shown in Fig. 7.23, whereas only a small amount of carbon deposition is detected during the machining with micro-MoS_2 particle-mixed dielectric. This is due to the decomposition of kerosene and attach to the machined surface. However, suspending MoS_2 maintains the high degree of dry lubricity since it is a dry lubricant. In addition, due to the increase in IEG, the MoS_2-mixed dielectric reduces the chance of arcing and short circuiting and increases the flushing efficiency; this in turn
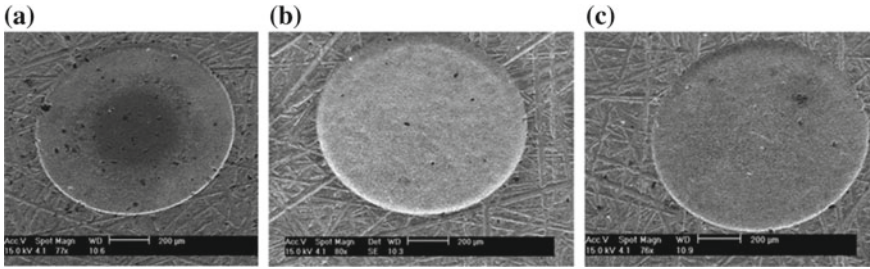
Fig. 7.23 **a** Pure dielectric, **b** dielectric with 2 g/l MoS$_2$, **c** dielectric with 5 g/l MoS$_2$ [21]. Study of workpiece vibration

reduces the carbon deposition and surface microcracks. Moreover, the high electrical conductivity of MoS$_2$-suspended fluid facilitates the increase in the IEG.

7.11 Research on PMμEDM

Tan and Yeo [25] have developed a numerical model to predict the surface characteristics of PMμEDM and estimated the plasma channel enlargement feature caused by the existence of powder particle in dielectric as 1.07 at 0.02 g/l of powder concentration. The comparison of results shown that PMμEDM model is sound. MoS$_2$ nanopowder (50 nm)-suspended dielectric was used to improve the fine finish of micro-EDM of Inconel 718 surface by Prihandana et al. [26]. The results showed that 5 g/l of powder concentration can achieve the better microholes and maximum material removal rate. Wang et al. [27] established that plasma channel in aluminium powder-mixed kerosene is more stable than pure kerosene and also found that stability increased with increase in current. Tiwary et al. [28] have compared the influence of various dielectrics, namely DEF-92, deionized water, and Cu powder-mixed deionized water during μEDM and shown that Cu powder in dielectric can significantly improve the performance μEDM in terms of MRR, TWR and OC.

Liew et al. [29] studied the effect of carbon nanofibre-suspended dielectric in μEDM on silicon carbide. Two types of EDM test (time controlling method and depth controlling method) were executed with various fibre concentrations. The electrosparking behaviour, MRR, EWR, electrode geometry, IEG, surface topography, and surface destruction were changed with the addition of carbon nanofibre in both tests. Suspension of carbon nanofibre improved the electrosparking rate of recurrence, MRR, and spark gap. Moreover, the form accuracy of microcavity and surface finish improved, and crater size reduced. Carbon nanofibre was moderately stick to the workpiece and prevented the material relocation among the electrode and workpiece.

Feasibility of improving the surface appearances in the PMμEDM of tungsten carbide with graphite nanopowder-suspended dielectric was investigated by Jahan et al.

[30]. Study on the enactment of powder-mixed μEDM was carried out, and surface characteristics were analysed in positions of surface features, crater characteristic, surface roughness (R_a), and peak to valley roughness (R_{max}). Spark gap, electrode wear and MRR were affected by graphite powder concentration. The surface finish and MRR were improved by the occurrence of graphite nanopowder in the dielectric, and EWR is reduced. For PMμEDM, the surface is uneven and imperfection-free related with sinking μEDM. But the material removal rate is maximum during the powder suspended sinking μEDM because of large area visible to machining. The average surface roughness and maximum peak to valley distance reduce as the powder concentration to certain limit thereafter increases as a result of powder settling as well as bridging of the IEG. For an optimum concentration of 2 g/L and voltage of 60 V, the lowest value of R_a and R_{max} was obtained for milling micro-EDM. The EWR also reduces with increase in powder concentration up to certain level and then increases.

Prihandana et al. [20] suspended nanographite particle in the dielectric with the application of ultrasonic vibration to overcome the powder settling issues and understood that it is an alternative to enhance the surface properties and to achieve faster machining. A technique by calculating the discharge pulse number has overcome the imprecision issues in nanographite PMD micro-EDM process. The suspension of nanopowder in dielectric fluid has abridged machining time by 35%. The upsurge in spark IEG and the increased powder percentage of nanographite in dielectric fluid affected the discharge to be further stable and decrease the requirement of retracting the tool electrode which results in reduced machining time. Moreover, nanopowder improved the machined surface integrity by reducing the chances of microcracks in the machined surface due to the uniform discharge distribution.

Jahan et al. [31] investigated the possibility of enlightening the R_a value of PMμEDMed tungsten carbide while graphite, aluminium, and alumina as the nanopowders. The effects of different powder characteristics were investigated analytically and experimentally and identified the existence of conductive or semiconductive powder lowered the dielectric strength of the dielectric, thereby larger IEG. Thus, the surface finish, MRR, EWR were found to be improved. The discharging process becomes more uniform, and thus, the craters become shallow. Semiconductive graphite powder can result in fault-free surface with better surface finish. Conductive aluminium powder gives higher spark gap and MRR. But nonconductive alumina powder did not show any significant effect on process performance.

In another study, Tan et al. [32] evaluated the recast layer thickness and identified the possibility for applying PMD on recast layer decrease and surface alteration. The process responses under various independent variables like particle concentration, nanosized particles, and sub-microsecond pulse on time duration were studied. SiC powder of powder granularity in the nanometre range and powder concentration of 5 g/L were used for the studies. The pulse on time of 606 ns provides longer interaction time and wider expansion of plasma channel. The electrode rotation speed of 1000 rpm generates thicker recast layer than 3000 rpm. The absorption of discharge energy by powder particle generates narrower melt pool, while the ease of

plasma channel expansion reduces plasma over pressure and facilitates molten material retention and overlapping recast layer formation.

The influence of SiC powder concentration in the dielectric and electric discharge energy in micro-EDM of Ti–6Al–4V with WC electrode is presented by Ali et al. [33]. Input variables were identified as SiC concentration, electric discharge energy. Addition of SiC powder reduces surface roughness up to a concentration of 20 g/l. The ANOVA shows that most influential factor on roughness is powder concentration, whereas electric discharge energy influences mostly on MRR and EWR. Cyril et al. [34] experimentally analysed the effect of powder concentration along with voltage, capacitance, feed, and rpm on various machining responses with aluminium, graphite, and silicon carbide-mixed dielectric fluid and found that a significant reduction in MRR and tool wear.

Yeo et al. [35] carried out single RC discharge experiments at different low discharge energies to study the effect of powder additives suspended in dielectric on crater characteristics for micro-EDM. Discharge energies of 2.5, 5, and 25 μJ were used. The crater formed is with small diameter and depth and has more consistent circular shape due to the presence of additives.

By studying the process using different dielectric fluids such as kerosene, kerosene with aluminium powder, and kerosene with SiC powder, Chow et al. [36] investigated the machinability of titanium alloy on micro-EDM. Addition of both powders to kerosene improves the material removal depth, discharge gap, and surface roughness. However, it is identified that material removal depth is found to be more for SiC powder while the significant improvement on surface roughness is for Al powder addition. Due to the largest gap obtained between electrode and workpiece, Al powder addition produces largest slit expansion. The EWR is increased due to the addition of powders which disturbs the adherence of carbon nuclides attached to the surface of electrode.

In another study, Chow et al. [37] investigated the microslit EDM process performance for Ti alloy using SiC powder in pure water as working fluid with small discharge energy. Conductivity of pure water increases with the addition of SiC powder, and thus, the discharge gap is increased. Due to the dispersion of discharge energy, surface roughness and MRR improved. Meanwhile, the addition of SiC to pure water increases the slit expansion and electrode wear than pure water.

7.12   Summary

Powder-mixed microelectric discharge machining is a growing day by day especially in the advanced micromachining of superalloys. To meet the requirement of miniaturization on the advanced materials and to overcome the processes inabilities of μEDM, PMμEDM is established as a viable and simple alternative. The improvements on the process capabilities mainly depend on the powder material properties, size, and its concentration in the dielectric. Generally, researchers have used conductive and semiconductive material powders. The presence of these external powders increases

the IEG and can produce better surface finish. This chapter mainly discussed the effect of powder particles in the dielectric on the working principle and its effect on various process responses. The effect of powders on the machined surface opens a new scope for exploring the possible μED alloying for the biomedical implants as a cheaper alternative where the conventional micromachining is not adequate. The research on various bio-inspired powder particles and its effect on the surface of bio-implants need to be addressed. In addition, a thorough research and development are also required to get the uniform recast layer on the surface to achieve the PMμEDM as a possible alloying technique. Hopefully, a few guidelines to achieve this transition were provided.

References

1. Kuriachen B, Mathew J (2016) Effect of powder mixed dielectric on material removal and surface modification in microelectric discharge machining of Ti-6Al-4V. Mater Manuf Process 31(4):439–446
2. Kansal HK, Sehijpal S, Kumar P (2007) Effect of silicon powder mixed EDM on machining rate of AISI D2 die steel. J Manuf Process 9:13–22
3. Paulom P, Elsa H (2008) Effect of the powder concentration and dielectric flow in the surface morphology in electrical discharge machining with powder-mixed dielectric (PMμ-EDM). Int J Adv Manuf Technol 37:1120–1132
4. Yeo SH, Tan PC, Kurnia W (2007) Effects of powder additives suspended in dielectric on crater characteristics for micro electrical discharge machining. J Micromech Microeng 17:91–98
5. Kunieda M, Lauwers B, Rajurkar KP, Schumacher BM (2005) Advancing EDM through fundamental insight into the process. CIRP Ann 54(2):64–87
6. Jahan MP, Wong YS, Rahman M (2009) A study on the quality micro-hole machining of tungsten carbide by micro-EDM process using transistor and RC-type pulse generator. J Mater Process Technol 209:1706–1716
7. Kumar S, Singh R, Singh TP, Sethi BL (2009) Surface modification by electrical discharge machining: a review. J Mater Process Technol 209:3675–3687
8. Klocke F, Lung D, Antonoglou G, Thomaidis D (2004) The effects of powder suspended dielectrics on the thermal influenced zone by electro-discharge machining with small discharge energies. J Mater Process Technol 149:191–197
9. Kansal HK, Sehijpal S, Pradeep K (2007) Technology and research developments in powder mixed electric discharge machining (PMEDM). J Mater Process Technol 184(1–3):32–41
10. Garg RK, Singh KK, Sachdeva A (2010) Review of research work in sinking EDM and WEDM on metal matrix composite materials. Int J Adv Manuf Technol 50:611–624
11. Jahan MP, Wong YS, Rahman M (2012) Experimental investigations into the influence of major operating parameters during micro-electro discharge drilling of cemented carbide. Mach Sci Technol 16:131–156
12. Mishra PK (2011) Nonconventional Machining. Narosa Publishing House, India
13. Kern R (2008) Sinker electrode material selection EDM today (July/August 2008 Issue)
14. Uhlmann E, Roehner M (2008) Investigations on reduction of tool electrode wear in micro-EDM using novel electrode materials. CIRP J Manuf Sci Technol 1:92–96
15. Fuller JE (1996) Electrical discharge machining. ASM Mach Handb 16:557–564
16. Wong YS, Lim LC, Lee LC (1995) Effects of flushing on electro-discharge machined surface. J Mater Process Technol 48:299–305
17. Karthikeyan G, Ramkumar J, Dhamodaran S, Aravindan S (2010) Micro electric discharge milling process performance: an experimental investigation. Int J Mach Tools Manuf 50(8):718–727

18. Klocke F, Lung D, Antonoglou G, Thomaidis D (2004) The effects of powder suspended dielectrics on the thermal influenced zone by electrodischarge machining with small discharge energies. J Mater Process Technol 149(1–3):191–197
19. Prihandana GS, Mahardika M, Hamdi M, Wong YS, Miki N, Mitsui K (2013) Study of workpiece vibration in powder-suspended dielectric fluid in micro-EDM processes. Int J Precis Eng Manuf 14(10):1817–1822
20. Prihandana GS, Mahardika M, Hamdi M, Wong YS, Mitsui K (2011) Accuracy improvement in nanographite powder-suspended dielectric fluid for micro-electrical discharge machining processes. Int J Adv Manuf Technol 56(1–4):143–149
21. Prihandana GS, Muslim M, Hamdi M, Wong YS, Mitsui K (2009) Effect of micro-powder suspension and ultrasonic vibration of dielectric fluid in micro-EDM processes-Taguchi approach. Int J Mach Tools Manuf 49(12–13):1035–1041
22. Wong YS, Lim LC, Rahuman I, Tee WM (1998) Near-mirror-finish phenomenon in EDM using powder-mixed dielectric. J Mater Process Technol 79(1–3):30–40
23. Kuriachen B (2015) Numerical modelling, simulation and experimental investigations of the micro electric discharge machining of Ti-6Al-4V, Ph.D. thesis submitted to National Institute of Technology Calicut, Kerala, India
24. Sanjeev K, Batra U (2012) Surface modification of die steel materials by EDM method using tungsten powder-mixed dielectric. J Manuf Process 14(1):35–40
25. Tan PC, Yeo SH (2013) Simulation of surface integrity for nanopowder-mixed dielectric in micro electrical discharge machining. Metall Mater Trans B 44(3):711–721
26. Prihandana GS, Sriani T, Mahardika M, Hamdi M, Miki N, Wong YS, Mitsui K (2014) Application of powder suspended in dielectric fluid for fine finish micro-EDM of Inconel 718. Int J Adv Manuf Technol 75(1–4):599–613
27. Wang X, Liu Y, Zhang Y, Sun Q, Li Z, Shen Y (2016) Characteristics of plasma channel in powder-mixed EDM based on monopulse discharge. Int J Adv Manuf Technol 82(5–8):1063–1069
28. Tiwary AP, Pradhan BB, Bhattacharyya B (2018) Investigation on the effect of dielectrics during micro-electro-discharge machining of Ti-6Al-4V. Int J Adv Manuf Technol 95(1–4):861–874
29. Liew PJ, Yan J, Kuriyagawa T (2013) Carbon nanofiber assisted micro electro discharge machining of reaction-bonded silicon carbide. J Mater Process Technol 213:1076–1087
30. Jahan MP, Rahman M, Wong YS (2011) Study on the nano-powder-mixed sinking and milling micro-EDM of WC-Co. Int J Adv Manuf Technol 53:167–180
31. Jahan MP, Rahman M, Wong YS (2010) Modelling and experimental investigation on the effect of nanopowder-mixed dielectric in micro-electrodischarge machining of tungsten carbide. Proc Inst Mech Eng [B] 224:1725–1739
32. Tan PC, Yeo SH (2011) Investigation of recast layers generated by a powder-mixed dielectric micro electrical discharge machining process. Proc Inst Mech Eng [B] 225(7):1051–1062
33. Ali MY, Atiqah N, Erniyati (2011) Silicon carbide powder mixed micro electro discharge milling of titanium alloy. Int J Mech Mater Eng 6(3):338–342
34. Cyril J, Paravasu A, Jerald J, Sumit K, Kanagaraj G (2017) Experimental investigation on performance of additive mixed dielectric during micro-electric discharge drilling on 316L stainless steel. Mater Manuf Processes 32(6):638–644
35. Yeo SH, Tan PC, Kurnia W (2007) Effects of powder additives suspended in dielectric on crater characteristics for micro electrical discharge machining. J Micromech Microeng 17:N91
36. Chow HM, Yang LD, Lin CT, Chen YF (2008) The use of SiC powder in water as dielectric for micro-slit EDM machining. J Mater Process Technol 195:160–170
37. Chow HM, Yan BH, Huang FY, Hung JC (2000) Study of added powder in kerosene for the micro-slit machining of titanium alloy using electro-discharge machining. J Mater Process Technol 101(1–3):95–103